Environ Monit Assess _####################_
https://doi.org/10.1007/s10661-019-7735-2

Temporal evolution of submicron particles during extreme fireworks

Sunil K. Yadav · Manish Kumar · Yashasvi Sharma · Prashant Shukla · Ram S. Singh · Tirthankar Banerjee

Received: 13 September 2018 / Accepted: 6 August 2019

Abstract Evolution of submicron particles in terms of particle number concentration and mobility-equivalent diameter was measured during Diwali festival–specific intensive pyrotechnic displays in Varanasi over central Indo-Gangetic Plain (IGP). A scanning mobility particle sizer coupled with an optical particle sizer was used to fit in an overlapping size range, and particle number concentration was analyzed to have an insight into the new particle formation and subsequent evolution of particles from nucleation to accumulation mode. Further, variation in black carbon (BC) concentration and aerosol ionic composition was measured simultaneously. Frequent fluctuation in particle number concentration in and around Diwali festival was evidenced, primarily influenced by local emission sources and meteorology, with three distinct peaks in number concentrations ($dN/d\log D_p$, 3.1–4.5 × 10^4 cm^3) coinciding well with peak firework emission period (18:00–23:00 h). Submicron particle size distribution revealed a single peak covering a size range of 80–130 nm, and for all instances, number concentration maximum coincided with geometric mean minimum, indicating the emission primarily in the ultrafine range (< 0.1 μm). Interestingly, during peak firework emissions, besides rise in accumulation mode, an event of new particle formation was identified with increase in nucleation and small Aitken mode, before being dispersed to background aerosols. On an integral scale, a clear distinction was noted between a normal and an episodic event, with a definite shift in the formation of ultrafine particles compared with the accumulation mode. The BC diurnal profile was typical, with a prominent nocturnal peak (12.0 ± 3.9 μg m^{-3}) corresponding to a decrease in the boundary layer height. A slight variation in maximum BC concentration (16.8 μg m^{-3}) was noted in the night of the event coinciding well with firework emissions. An increase in some specific ionic species was also noted in combination with an increase in the overall cation to anion ratio, which was explained in terms of heterogeneous transformation of NOx and catalytic conversion of SO_2.

Keywords Diwali · Fireworks · Nucleation · Particle evolution · Ultrafine particles

Electronic supplementary material The online version of this article (https://doi.org/10.1007/s10661-019-7735-2) contains supplementary material, which is available to authorized users.

S. K. Yadav · P. Shukla
Department of Mechanical Engineering, Indian Institute of Technology (BHU), Varanasi, India

M. Kumar · T. Banerjee (✉)
Institute of Environment and Sustainable Development, Banaras Hindu University, Varanasi 221005, India
e-mail: tb.iesd@bhu.ac.in

e-mail: tirthankaronline@gmail.com

Y. Sharma · R. S. Singh
Department of Chemical Engineering and Technology, Indian Institute of Technology (BHU), Varanasi, India

R. S. Singh · T. Banerjee
DST-Mahamana Centre of Excellence in Climate Change Research, Banaras Hindu University, Varanasi, India

Introduction

Aerosols are multi-component mixtures that originate from different sources and evolve through several microphysical processes like nucleation, coagulation, and condensation, before being removed through dry or wet deposition (Banerjee et al. 2015). Aerosols are important constituents of the earth's atmosphere, which either directly or indirectly influence climate, air quality, visibility, and human health (Lelieveld et al. 2015; Kumar et al. 2015; Goel and Kumar 2015). Additionally, aerosols are also linked with modification in cloud microphysical properties (Gettelman et al. 2013), hydrological cycle (Ramanathan et al. 2001), radiative forcing (Kumar et al. 2017a, b), and with food security (Burney and Ramanathan 2014). The effects of aerosols on human health are of serious concern (Burnett et al. 2018), particularly for nations with very fast-changing economies (India and China). Therefore, understanding aerosol formation and its evolution from submicron to coarse particulates is of great importance to atmospheric researchers.

Evolution of airborne particulates and its physico-chemical properties is a function of aerosol sources and meteorology (Kumar et al. 2016; Murari et al. 2016; Singh et al. 2003). Recently, primary sources of fine particulates over South Asian region were reviewed by Singh et al. (2017), which comprehended vehicular emissions to be the most dominating one, followed by industrial emissions and secondary aerosols. However, apart from these established emission sources, some typical exogenous factors like extensive fireworks also possess potential to substantially modify the local-to-regional aerosol and therefore, they are widely explored in scientific literature (Devara et al. 2015; Kumar et al. 2016; Moreno et al. 2007; Zhao et al. 2017; Joshi et al. 2016). Extensive fireworks during major celebratory events are rather common across the world. Over the Indian subcontinent, Diwali—the festival of light is a kind of event commonly celebrated with burning illuminations and firecrackers on a large scale. Celebratory events in other parts of the world with large-scale fireworks, i.e., the Independence Day celebration in the USA, New Year's Eve in Europe, and Lantern Festival in China, are also reported with huge emissions of airborne particulates (Retama et al. 2019; Lin et al. 2014). This unique kind of source generates massive amount of pollutants within a very short time (Sarkar et al. 2010; Kumar et al. 2016) and contributes to an increase in the background pollution. In our earlier submission, we characterized the spatio-temporal nature of particulate emissions over the Indo-Gangetic Plain (IGP) during Diwali festival, and an increase of 56–121% of particulate loading was noted over background concentration. Further, satellite-retrieved columnar aerosol properties established the dominance of absorbing aerosols with a strong vertical gradient of smoke aerosols. Even there was evidence of gas-to-particle conversion on subsequent days leading to an increase in concentration of coarser particulate (Kumar et al. 2016).

The emission of particulates during any major celebratory events is widely discussed in the literature. Often such emissions are linked with the poor ambient air quality (Seidel and Birnbaum 2015; Vecchi et al. 2008; Wang et al. 2007), changes in particulate composition (Perrino et al. 2011; Kumar et al. 2016; Deka and Hoque 2014), and impacts on human health (Becker et al. 2000; Thakur et al. 2010; Kumar et al. 2015), while few have also investigated their impacts on columnar aerosol properties and aerosol vertical profile (Singh et al. 2003; Devara et al. 2015; Kumar et al. 2016). Almost all the studies have established the increase in the aerosol concentrations during fireworks, with increase in firework-specific tracers like P, K, Mg, Cu, and S. However, scientific understanding regarding the evolution of particulates, especially from nucleation to accumulation mode is limited as only few studies have explored the change in particulate number concentration and size distribution, especially in the submicron stage. Despite contributing the most mass and number concentrations to the total aerosols and having associated negative health impacts, limited information is available in terms of evolution and dynamics of submicron particles. There are evidences of eventual increase in accumulation mode particles from nucleation and small Aitken mode (Jing et al. 2014; Zhang et al. 2010; Zhao et al. 2017; Joshi et al. 2016), while on the contrary, some researchers have also documented a significant increase in ultrafine particles during fireworks (Wen and Chen 2013; Joshi et al. 2016). In India, Singh et al. (2003, in Kanpur) and Joshi et al. (2016, in Mumbai) addressed the evolution of submicron particles during Diwali festival fireworks and reported an increase in the total number concentrations, especially in ultrafine mode. However, both experiments were unable to present any conclusive evidence in distinguishing an episodic and a normal event due to the concurrent influence of other

anthropogenic emissions and due to unavailability of the aerosol chemical composition. Considering these uncertainties, the number size characteristics of airborne submicron particulates emitted from extensive fireworks were analyzed to get an insight into the evolution of particulates from nucleation to the accumulation stage. Further, the diurnal variation in black carbon (BC) and particulate-bound ion concentration anomalies with respect to baseline concentration is also reported.

Experimental methods

Sampling site

The experiment was conducted in Varanasi (25° 16′ N, 82° 59′ E), an inland station within central IGP having a high background aerosol concentration throughout the year (Kumar et al. 2017a, b; Murari et al. 2015; Mhawish et al. 2017, 2018; Sen et al. 2017). Figure 1 indicates the ground monitoring location with a background of surface reflectance retrieved from Visible Infrared Imaging Radiometer Suite (VIIRS) satellite on October 31, 2016, which typically indicates the presence of a huge aerosol layer, especially over northern parts of India. Particulate measurements were made within the premises of the Indian Institute of Technology (IIT-BHU) campus at a height of 25 m to attain the appropriate background aerosol concentration (Zhao et al. 2017). Monitoring was carried out for 5 days (October 28–November 2, 2016) from 12:00 to 12:00 h, with the celebratory event falling on October 30, 2016. The sampling location represents academic premises with no direct influence of industrial and vehicular emissions.

Particulate measurement

A scanning mobility particle sizer (NanoScan SMPS Nanoparticle Sizer3910, TSI, USA) and an optical particle sizer (OPS 3330, TSI, USA) were used to measure the particulate number concentration and the particle size distribution. Both the NanoScan SMPS and the OPS were used in conjunction to measure the size of particles in the range of 10 nm–10 μm. The NanoScan works on the principle of the particle mobility and OPS works on the principle of light scattering. The NanoScan SMPS was used to measure the particle size distribution between 10 and 420 nm with a sampling flow rate of 0.8 l/min covering 13 size bins, while OPS was used to measure particle size distribution between 300 and 10,000 nm with a sampling flow rate of 1 l/min covering 16 size bins. Additional QA/QC details of both the instruments are available elsewhere (Yamada et al. 2015; Tritscher et al. 2015). The time resolution of both particle sizers was 1 min. The mean mobility-equivalent diameter and particle number concentrations on an hourly basis were calculated by averaging 1-min resolution data for each size bins. Further, particle number for every size bins for every respective hour were added to obtain the total particle number for each mode, i.e., nucleation (10–20 nm), small Aitken (20–50 nm), large Aitken (50–100 nm), and accumulation (100–1000 nm). Aerosols were sampled without any drying arrangement. It is to be mentioned that an insignificant number of particles were observed above 1000-nm size range in comparison with the lower size ranges. Hence, the particle size distribution above 1000 nm was not included in the analysis.

In addition to this, in situ measurement of airborne particulates having aerodynamic diameter (d_{ae}) of ≤ 2.5 μm ($PM_{2.5}$) was also concurrently made with the help of a fine dust sampler (APM-550, Envirotech) (flow rate, 1 m^3 h^{-1}; accuracy, ± 2%) using polytetrafluoroethylene filters (PTFE, 47 mm dia.) on a 24-h basis (12:00 to 12:00 h). PTFE filters were desiccated for 24 h before and after sampling, and the particulate mass concentrations were estimated gravimetrically. The exposed filters were stored under cool and dry conditions (− 20 °C) for chemical analysis. Details regarding particulate collection, analysis, and quality control may be found in the work of Murari et al. (2017).

Black carbon aerosols

Real-time aerosol BC mass was measured using a seven-channel aethalometer (AE 42: Magee Scientific Company, USA) having a 5-min temporal resolution. The estimation of BC mass loading is based on the attenuation of light transmitted at a specific wavelength (880 nm). The attenuation of light is a function of aerosol mass being deposited on the filter tape by a uniform air with a flow rate of 3 LPM. The aethalometer converts light attenuation (ATN) into BC mass concentration using a fixed specific attenuation cross-section (σ) of 16.6 m^2 g^{-1} of BC. The linearity between BC mass and light ATN was used to modify during high

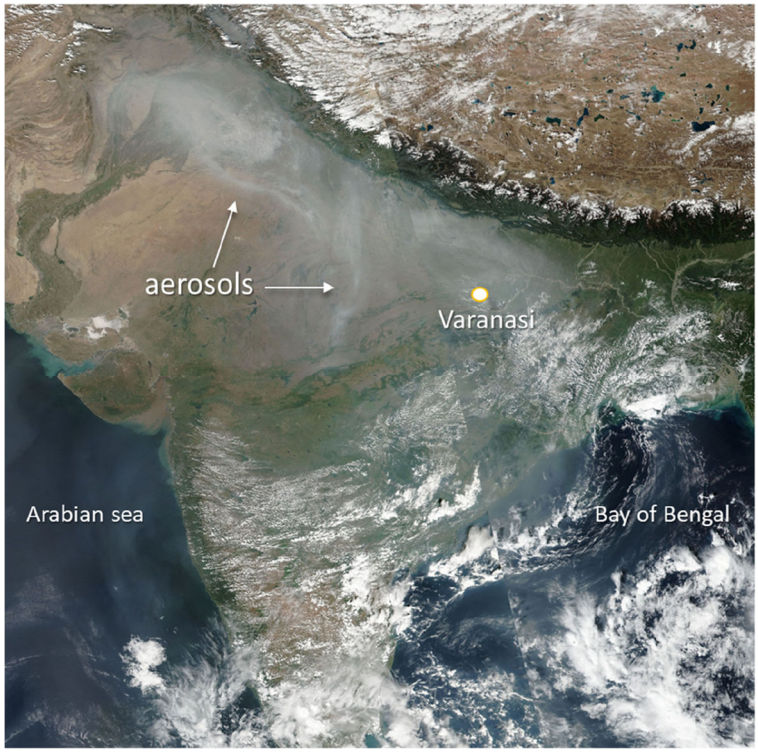

Fig. 1 Geographical location of aerosol monitoring station. Note: Background image retrieved from VIIRS satellite indicates the thick aerosol layer over north India on October 31, 2016

deposition of BC aerosols (Hansen et al. 1984), and hence results into a reduced BC mass concentration (loading or shadowing effects). This was eventually removed using an empirical correction algorithm proposed by Virkkula et al. (2007).

Aerosol ionic composition

Ionic species present in fine aerosols were analyzed through an ion chromatograph. The collected $PM_{2.5}$ samples were extracted in deionized water using an ultrasonicator bath (Microclean-109, Oscar, India). The samples were analyzed for major anions (F^-, Cl^-, NO_3^-, SO_4^{2-}) and cations (Na^+, K^+, NH_4^+, Mg^{2+}, and Ca^{2+}) using ion chromatograph (ICS-3000, Dionex, USA). The anions were estimated using an anion micromembrane suppressor (AERS-300, 4 mm; Dionex, USA) with IonPac analytical column (AS11-HC, 4 × 250 mm) connected with guard column IonPac (AG11-HC, 4 × 50 mm; Dionex, USA), while the cations were analyzed using suppressor (CERS-300, 4 mm; Dionex, USA) with an analytical column (IonPac CS12A-HC, 4 × 250 mm; Dionex, USA) associated with a guard column (IonPac CG11-HC, 4 × 50 mm; Dionex, USA). Details about the preparation of samples and instrumentation can be found in our previous works (Sharma et al. 2014; Kumar et al. 2017a, b).

Results and discussion

Time-series of particle number concentration

Figure 2 indicates the time series of particulate number concentration and corresponding geometric mean diameter for the entire monitoring period. During the Diwali festival, fireworks typically peak at late evening up to midnight (19:00–23:00 h), and celebrations during pre- and post-Diwali days are also very common. In our previous submission, late-night and post-Diwali intensification of fine particulates indicated the presence of accumulation mode particles (Kumar et al. 2016). Therefore, in order to understand the diurnal and pre-to-post Diwali variation and to make it consistent with the monitoring duration of fine particulate sampler, aerosol measurements from 12:00 to 12:00 h were considered as an individual day. The monitoring period was subsequently divided into three based on expected aerosol loadings/formation in and around Diwali festival: pre-Diwali days (D-2, D-1: October 28–30), the Diwali

day (D: October 30–31), and post-Diwali days (D+1, D+2: October 31–November 02).

Figure 2 clearly indicates the frequent fluctuations in particle number concentration ($dN/d\log D_p$; range, 0.28–6.07 × 10^4; average, 1.67 × 10^4 cm^{-3}) in and around Diwali, with three distinct cases (peaks A, B, C) of massive increase in particle number concentrations. Apart from these three, there are few minor repeated peaks, which may well have been influenced by local emissions and/or favorable meteorological conditions and due to the low condensation sink (Zhao et al. 2017). The most prominent increase in particle concentration appeared on the night of the event (peak B) during 18:00-23:00 h, with an average hourly particle number concentration of 4.5 × 10^4 cm^{-3}, having mean mobility-equivalent diameter of 89.5 nm. The remaining two peaks (A, C), with relatively lower intensities, coincide well with pre- (D-1) and post-celebratory (D+1) firework emissions. Both the peaks were evident on a similar time frame (18:00–23:00 h) with almost similar average particle number concentration (D-1, 3.1 × 10^4; D+1, 3.2 × 10^4 cm^{-3}) and mean particle diameter (D-1, 89.0; D+1, 100.0 nm). In all instances, the maximum values in number concentration coincided with the minimum geometric mean (for the entire size range) signifying the emission to be in the ultrafine range (< 100 nm). Another distinct feature that emerged was the occurrence of consistent repetitive peaks (marked with red arrow) during early morning hours (07:00–9:00 h, ± 1 h), with moderate particle number concentration ($dN/d\log D_p$, 1.5–2.7 × 10^4 cm^{-3}) that coincides with the subsequent decrease in the particle mean diameter. Such moderate increase in particle number concentration and subsequent decrease in mobility-equivalent diameter indicate the formation of ultrafine particles which ultimately increases the particle number (Joshi et al. 2016).

In order to better understand the size distribution of submicron aerosol particles during fireworks, the daily mean particle number size distributions ($dN/d\log Dp$) representing the particle number concentrations in each channel for the overall size range are plotted in Fig. 3. The submicron particle size distribution exhibits a single peak effectively covering a size range of 80–130 nm and indicates dominance of large Aitken and accumulation mode particles. Aerosol concentrations were clearly high on the eventful day (D) for almost all the size range, followed by pre- and post-Diwali days. The 24-h average particle number concentration was unable to identify any clear shift in the particle size distribution during extreme fireworks, except recognizing a moderate increase in small and large Aitken mode particles. However, in comparison with non-episodic days, nucleation mode particle accounted the highest increase on Diwali day (% increase: D-2, 219%; D+2, 153%) (Table S1, in supplementary file), invariably suggesting the formation of new particle during fireworks, which gradually coagulate and become part of background aerosols (Dal Maso et al. 2005; Zhao et al. 2017).

To gain a deeper insight into the particle formation, the integral particle number concentration in four individual modes was compared on a shorter time frame (4-h time frame), for all the monitoring days, and presented in Table 1. Selection of this time frame was ideally to separate changes in atmospheric characteristics due to specific events like fireworks and/ or any meteorology and was in accordance with Kumar et al. (2016) and Joshi et al. (2016). As expected, a shorter time frame in number concentration was able

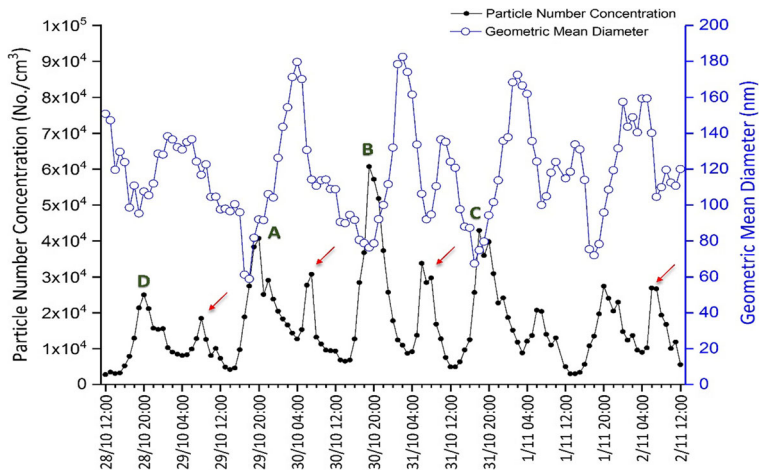

Fig. 2 Time series of particulate number concentration and geometric mean diameter

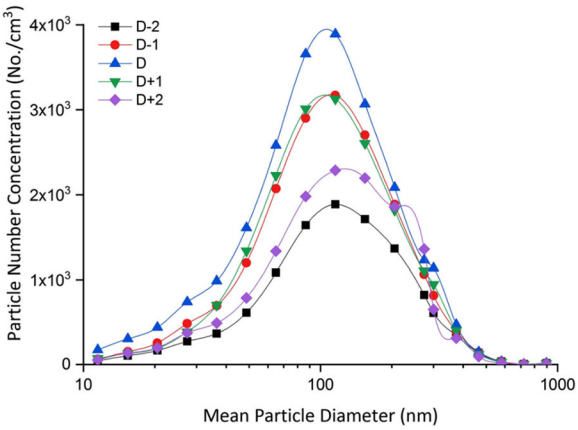

Fig. 3 Daily mean particle number size distributions during days of the study

to resolve the periodic evolution of particles under both firework-dominated and normal conditions. A massive increase in the number concentration of nucleation and small Aitken mode particles on the night of the event was observed, especially during 16:00–24:00 h, apart from the general increase in accumulation mode. During peak firework emission on the day of Diwali festival (16:00–20:00; 20:00–24:00 h), nucleation (502, 144%), and small Aitken (285, 172%) mode particles registered a sudden flush of generation (against D-2), which was otherwise not evident on the normal days. Overall, a marked change in generation of ultrafine particle was noted and was therefore compared with accumulation mode particles to recognize any consistency in particle evolution. In a continuous time series, Fig. 4 compares the 4-h averaged variation in ultrafine particle number concentration with accumulation mode particles, and a clear indication of particle evolution was noted (marked with red arrow) for all firework-dominating episodes. During intensive firework emissions, especially from 18:00–23:00 h (for D, D-1, D+1), a clear and persistent increase in ultrafine particles was recorded followed by subsequent growth in accumulation mode particles. This was in contrast to the normal events (D-2, D+2) where generation of ultrafine and accumulation mode particles was almost in parallel (marked with black arrow).

Table 1 Particle size distribution characteristics averaged over 4 h

Time block	Study day	Nucleation mode (10–20 nm)		Small Aitken mode (20–50 nm)		Large Aitken mode (50–100 nm)		Accumulation mode (100–1000 nm)	
		N_t (No./cm^3)	GMD (nm)	N_t (No./cm^3)	GMD (nm)	N_t (No./cm^3)	GMD (nm)	N_t (No./cm^3)	GMD (nm)
16:00–20:00	D-2	428.19	16.38	1957.70	37.13	3127.00	77.11	6319.45	208.13
	D-1	1261.23	17.46	5738.39	40.00	7778.49	77.17	8809.51	178.13
	Diwali	2577.78	17.33	7537.12	38.31	10675.65	78.41	13847.49	186.39
	D + 1	848.86	16.68	6480.60	40.53	11168.76	76.66	10730.96	175.61
	D + 2	924.97	17.00	3033.23	37.15	3114.17	76.15	5284.26	186.91
20:00–24:00	D-2	592.46	16.26	2188.35	37.93	4752.40	76.80	11744.62	206.57
	D-1	705.10	17.52	3986.73	39.65	8934.81	77.59	15706.85	184.48
	Diwali	1446.38	17.49	5960.98	38.09	12190.82	78.21	23394.72	188.70
	D + 1	548.14	16.56	3003.56	40.40	7771.98	76.70	18062.67	172.46
	D + 2	520.96	17.02	2157.88	37.04	5085.88	75.69	15946.85	180.75
24:00–04:00	D-2	152.59	16.70	524.98	38.43	2480.33	76.37	7647.93	201.50
	D-1	104.19	17.63	302.31	39.94	3072.02	78.00	13909.51	186.26
	Diwali	245.77	17.06	319.02	37.96	1446.23	77.97	10431.85	191.54
	D + 1	101.14	16.38	186.40	39.89	2003.49	76.46	11283.96	173.24
	D + 2	121.01	16.89	449.72	37.86	2425.37	75.44	9563.15	171.07
04:00–08:00	D-2	284.65	16.96	919.49	38.99	2082.65	76.41	6464.91	191.46
	D-1	288.39	17.58	1779.24	39.55	5822.06	78.45	13697.04	187.49
	Diwali	376.49	17.29	3473.51	37.86	6769.81	77.61	10050.97	191.78
	D + 1	344.83	16.47	2061.34	39.07	4579.01	76.45	9699.54	180.59
	D + 2	328.13	16.82	1860.32	39.13	4831.34	75.39	11155.74	161.62

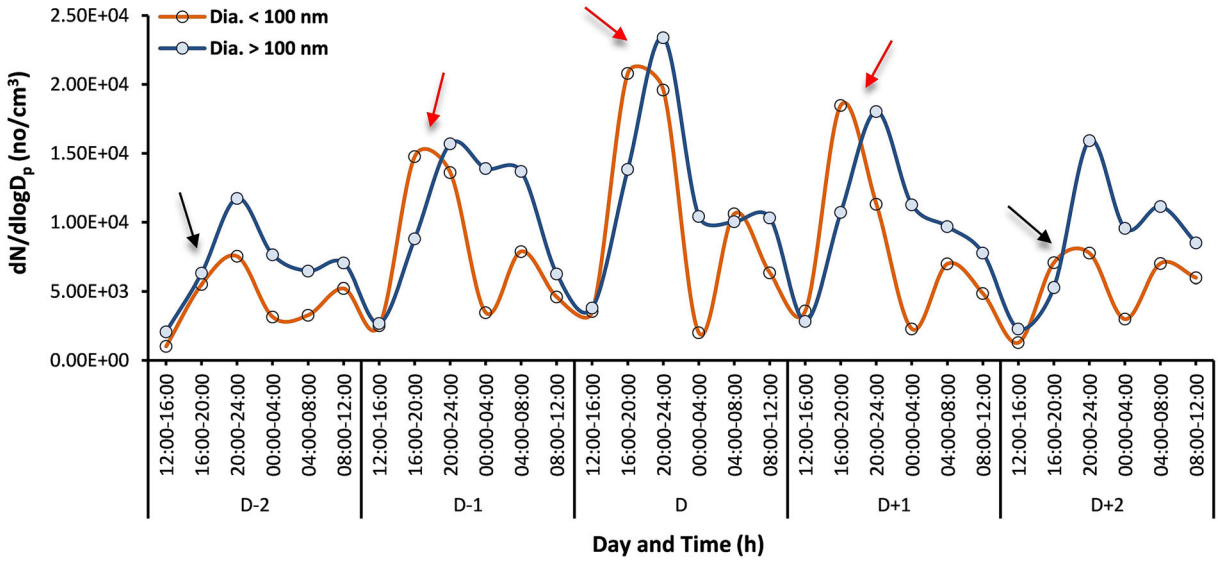

Fig. 4 Time series of ultrafine and accumulation mode particle number concentrations

This certainly indicates that the new particles that form during fireworks, which gradually evolve to a larger size, further disperse into the natural environment. This also eventually establishes the fact that during extreme fireworks, generation of ultrafine particles mostly happens in nucleation and Aitken mode, which significantly increases with a shifted accumulation peak.

Comparison of episodic and background event

Beside comparing long- and short-term variations in particle number concentration and providing insight into particle size distribution, we also analyzed the evolution of individual peaks that appear during firework and non-firework days. Time-resolved (1 h) evolution of a single peak that directly represents firework emissions was compared against a background peak (maybe in different magnitude), to understand any possible discrepancy in particle evolution. Integral size distribution measurement corresponding to 18:00 to 23:00 h was selectively considered owing to the highest firework emissions. As evident in Fig. 2, peaks appeared during extreme fireworks (A, B, C) differ only in magnitude; however, we considered only peak B (the highest; $dN/d\log Dp$, 4.5×10^4 cm^{-3}; GMD, 89.5 nm) to compare against peak D (1.86×10^4 cm^{-3}; GMD, 110.0 nm), which appears to be less influenced by firework emissions. Both peaks were considerably different in terms of magnitude and mean mobility-equivalent diameter and also exhibit a contrasting pattern in terms of their evolution (Fig. 5). In case of peak B, generation of two additional modes at nucleation (< 20 nm) and small Aitken stage (20–50 nm) was also noted during 19:00–20:00 h, which coincides precisely with peak firework emission, before being coagulated into large Aitken mode. Peak evolution characteristics continued to show the identical trend till 23:00 h, although to a varying extent. Overall, additional modes in nucleation and Aitken stages were noted followed by an accumulation mode. In contrast, the evolution of particle size distribution for a normal event (peak D) was much smoother, with number concentration for all size ranges increased laterally without having any specific peaks at < 50 nm. The mobility-equivalent mean particle diameter was comparatively high (110.0 nm) which indicate the presence of accumulation mode particles. This concludes the overall argument that fireworks essentially emit ultrafine particles, having a significant proportion of such particles falling under nucleation and small Aitken modes, which gradually evolve through coagulation and contribute to the background aerosols.

Variation in black carbon aerosols

The diurnal variations in BC aerosols are presented in Fig. 6 with a comparison of 24-h mean BC concentration for all the monitoring days. The BC diurnal profile was typical to the central IGP, with a daytime low (7.3 ± 3.5 μg m^{-3}) and nighttime high concentration (12.0 ± 3.9 μg m^{-3}). Despite having any night-specific BC

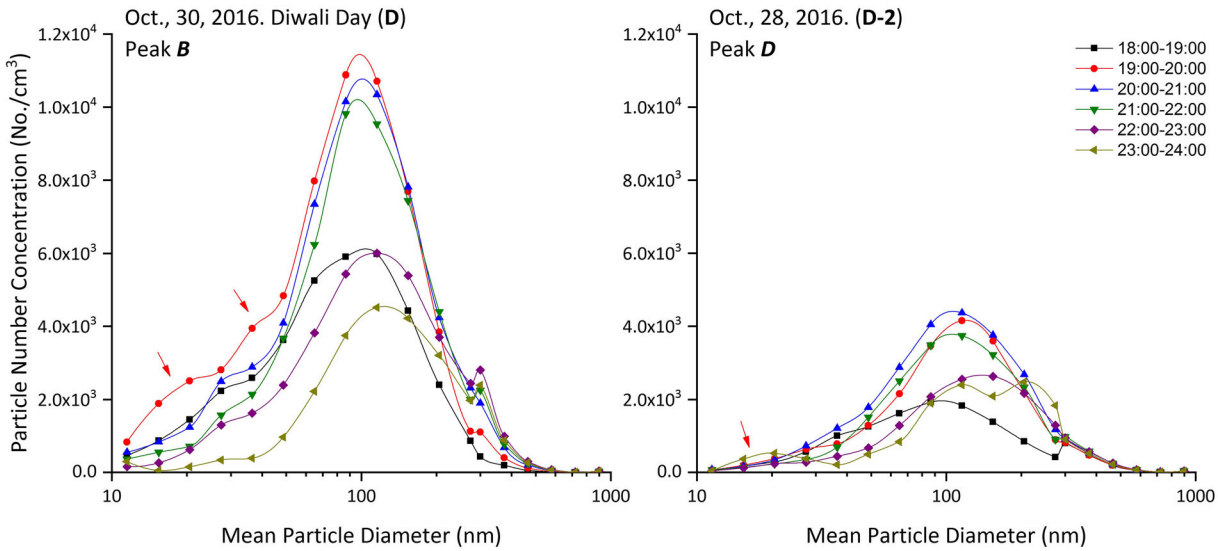

Fig. 5 Time resolved evolution of particle size distribution during normal and episodic events

emission sources, such characteristic increase is linked with local meteorology, especially with the boundary layer height (Kumar et al. b). Since the prevailing wind speed was calm (Table S2), changes in atmospheric boundary layer depth over the day (mean ± SD, 963 ± 828 m) and night (50 ± 0 m) possibly affect the diurnal variation of BC. The 24-h (12:00–12:00 h) average BC concentration varied between 7.2 and 11.5 μg m^{-3}, with an hourly peak value of 22.0 μg m^{-3}, having an insignificant difference within pre- and post-celebrations against Diwali day. Average pre-Diwali BC concentration was 10.6 ± 4.7 μg m^{-3}, which was also most equivalent to Diwali day (10.3 ± 4.6 μg m^{-3}), before reducing to 8.1 ± 3.6 μg m^{-3} during post-Diwali. Such decreasing trend in BC mass loading was identical to our prior observations for a similar location reported by Kumar et al. (2016). The monitoring site is located in the central part of IGP, with high background

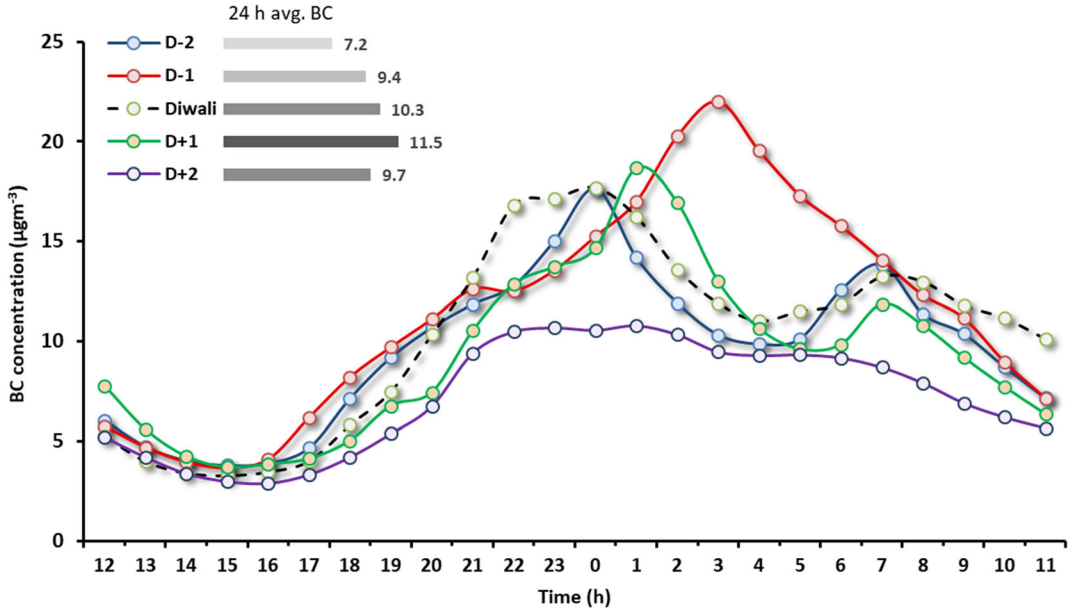

Fig. 6 Diurnal variation of black carbon concentration (μgm^{-3})

concentrations of BC aerosols mainly emitting from vehicular emissions (Kumar et al. 2017a, b). The insignificant decrease in BC concentration in spite of firework emissions is assumed to be associated with the suppression of background activities, like vehicular and industrial emissions, which ultimately reduces the total BC concentration. Our observations were in line with the findings of Sarkar et al. (2010), where a reduction in vehicular emissions during Diwali day in Delhi was reported to be responsible for the overall reduction in BC.

Usually, maximum BC concentration lies between 24:00 and 04:00 h for all the normal days, while on the Diwali day, the period shifted slightly to 21:00–24:00 h, coinciding well with the maximum firework emissions. A gradual increase in BC concentrations from 17:00 h coincides well with the peak traffic hours, after which BC gets accumulated in the lower atmosphere by virtue of low wind speed and a net reduction of boundary layer height. Such characteristic behavior in BC accumulation in the lower troposphere is similar to airborne particulates, which also get trapped in the lower atmosphere by the reduction in mixing height (Murari et al. 2017). The size distribution of internally mixed BC particles lies around ~ 230 nm for condensation mode mainly consisting of traffic emissions and around ~ 380 nm for droplet mode (highly aged traffic emission and biomass burning particles) (Gong et al. 2016). Firework-induced BC emissions typically mix internally with K, ammonium sulfate, and ammonium nitrate; therefore, they resemble the traffic-induced BC emissions and contribute to the total particle number concentrations within accumulation mode.

Variations in particle ionic composition

On account of the evolution of several particles during the fireworks in potentially respirable range, fine particles ($PM_{2.5}$) were collected for analyzing selected water-soluble inorganic components (WSIC). The majority of firework-induced particles being inorganic in nature (Liu et al. 1997), the investigation of particle-bound elements and ionic species is a prerequisite to reveal their toxicological implications. A significant rise in particulate elemental concentrations for a similar site is already reported (Kumar et al. 2016). Hence, the current assessment was only limited to WSIC.

The multifold increment (K+, 527%; Mg2+, 175%; NO3-, 57%; Cl-, 291%, Table S3) in firework-specific ionic mass from pre-Diwali (D-2) to Diwali day depicts the contribution of firework emission of WSIC to ambient aerosols. Nitrates, chlorates, and perchlorates of potassium are used as oxidizers in the firecrackers, while nitrates and chlorates of barium are used as a coloring agents. In combination, K+, Cl-, and NO3- contribute 60% of total WSIC mass, while a higher increase in Cl- concentration compared with that in NO_3^- possibly indicates the choice of chlorates and perchlorates as firework oxidizers over nitrates. Variations in micro-equivalents of ionic species reveal a changing pattern with a cation to anion ratio (C/A) remaining > 1 (Fig. 7). However, it sharply varied during pre- (D-1, 1.7; D-2, 2.0), post (D+1, 1.7; D+2, 1.2), and on Diwali day (D. 2.4), with corresponding changes in the emission. The significant changes in positive ions, i.e., K^+, Mg^{2+}, and NH_4^+, during firework emissions are attributed to the modification in the C/A ratio. A sharp rise in micro-equivalents of anionic species (NO_3^- and Cl^-) was also observed but lagged before their cationic counterparts. The formation of nitrate was mainly through homogenous gas-phase reactions of NO_2, while the presence of Cl^- indicates its extensive use as coloring agent, and formation of chloride salt of K, Mg, Ba, Pb, and Sr during fireworks (Wang et al. 2007).

The micro-equivalent ratio of total cation to anions changed immediately after Diwali with sudden increase in anionic micro-equivalents. The increment in anionic micro-equivalents during post-Diwali days is chiefly dominated by an increase in SO_4^{2-} concentrations due to slow heterogeneous catalytic transformations of SO_2 to SO_4^{2-} particle (Wang et al. 2007). Sulfur is commonly used as an additive in gunpowder for explosion. However, the slow rate of conversion of SO_2 to SO_4^{2-} during winter (0–2.8% per hour; Cheng et al. 1987) facilitates the conversion of SO_2 at upwind location and gradual accumulation over the central Gangetic plain after days of emissions.

Conclusions

The number size characteristics of submicron particulates emitted from Diwali -festival of light specific

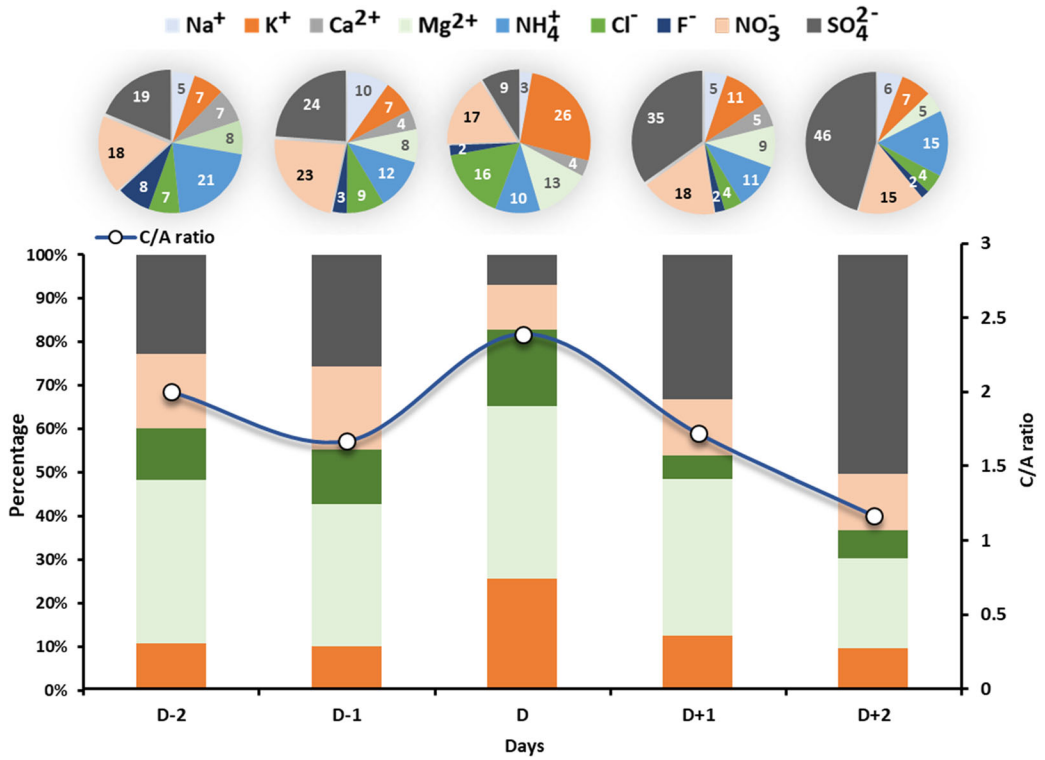

Fig. 7 Variations in particulate ionic compositions, with equivalent concentration of K^+, Mg^{2+}, Cl^-, NO_3^- and SO_4^{2-}, and cation-to-anion ratio

extensive fireworks were investigated in Varanasi. Emphasis was made to get an insight into the formation and evolution of particle from nucleation to accumulation mode. A comparison of aerosol chemical composition in terms of particulate-bound ion was also made. Additionally, diurnal variations in black carbon (BC) aerosols with respect to baseline concentration were also analyzed. The important findings of the study are summarized as:

(a) Overall time series of particle number concentration revealed a clear signature of firework-specific increase (153–219%) in ultrafine particle concentration and corresponding changes in mobility-equivalent diameter. The hourly averaged particle number concentration on Diwali day reaches as high as 4.5×10^4 cm^{-3} with a mean mobility-equivalent diameter of 89.5 nm.

(b) On integral scale, a clear discrepancy was noted between a normal and episodic event, with a definite shift in ultrafine particle formation compared to that in accumulation mode. A clear indication of new particle formation was evidenced on Diwali festival night (16:00–24:00 h) and somewhat during pre- to post-Diwali celebrations, with a sudden massive increase in the formation of nucleation and small Aitken mode particles, which consequently coagulate and contribute to the background aerosols.

(c) The BC aerosol time series followed typical characteristic of the central IGP, with daytime low (7.3 ± 3.5 μg m^{-3}) and nighttime high concentration (12.0 ± 3.9 μg m^{-3}), which was explained in terms of variation in atmospheric boundary layer height. The overall variation in average 24-h BC concentration from pre- to post-Diwali was insignificant.

(d) Ionic composition of fine particulates revealed an increase in firework-specific tracers (K^+, Mg^{+2}, NO_3^-, Cl^-) from pre-Diwali to Diwali day. Nitrate was mainly formed through homogeneous gas-phase reactions of NO_2, while an increase in SO_4^{-2} concentrations was only evident in post-

Diwali due to heterogeneous transformations of SO_2 into SO_4^{-2} particle.

(e) The cation-to-anion ratio remained > 1 throughout the study period; however, very high C/A ratio (2.4) on Diwali day indicates dominance of firework-specific cations (K^+, Mg^{+2}) in the airborne particulates.

There were some limitations of the experiment as the volume of air sampled for measuring particle number concentration may not be an actual representation of the outdoor environment. Besides, an active humidity controller and diluter were needed to be assembled with NanoScan SMPS and OPS for accurate outdoor monitoring.

Funding information This work was financially supported by the Bhabha Atomic Research Centre, Mumbai (No. 2013/36/67-BRNS/0577). Black carbon was monitored under Aerosol Radiative Forcing over India (ARFI) scheme (P-32-13) financed by Indian Space Research Organization, Thiruvananthapuram. MK acknowledges the Council for Scientific and Industrial Research (CSIR) for Senior Research Fellowship.Data availabilityThe VIIRS land surface reflectance is available at NASA's EOSDIS Worldview.

Compliance with ethical standards

Conflict of interest The authors declare that they have no conflict of interest.

References

Banerjee, T., Murari, V., Kumar, M., & Raju, M. P. (2015). Source apportionment of airborne particulates through receptor modeling: Indian scenario. *Atmospheric Research, 164*, 167–187.

Becker, J. M., Iskandrian, S., & Conkling, J. (2000). Fatal and near-fatal asthma in children exposed to fireworks. *Annals of Allergy, Asthma & Immunology, 85*, 512–513.

Burnett, R., Chen, H., Szyszkowicz M et al. (2018). Global estimates of mortality associated with long-term exposure to outdoor fine particulate matter. Proc Natl Acad Sci USA, 115, 9592–9597.

Burney, J., & Ramanathan, V. (2014). Recent climate and air pollution impacts on Indian agriculture. *PNAS, 11*, 16319–16324.

Cheng, L., Peake, E., & Davis, A. (1987). The rate of SO_2 to sulfate particle formation in an air parcel from an oil sands extraction plant plume. *JAPCA, 37*, 163–167.

Dal Maso, M., Kulmala, M., Riipinen, I., Wagner, R., Hussein, T., Aalto, P. P., & Lehtinen, K. E. (2005). Formation and growth of fresh atmospheric aerosols: eight years of aerosol size distribution data from SMEAR II, Hyytiala, Finland. *Boreal Environment Research, 10*, 323–336.

Deka, P., & Hoque, R. R. (2014). Diwali fireworks: early signs of impact on PM10 properties of rural Brahmaputra valley. *Aerosol and Air Quality Research, 14*, 1752–1762.

Devara, P. C., Vijayakumar, K., Safai, P. D., Made, P. R., & Rao, P. S. (2015). Celebration-induced air quality over a tropical urban station, Pune, India. *Atmospheric Pollution Research, 6*, 511–520.

Gettelman, A., Morrison, H., Terai, C. R., & Wood, R. (2013). Microphysical process rates and global aerosol–cloud interactions. *Atmospheric Chemistry and Physics, 13*, 9855–9867.

Goel, A., & Kumar, P. (2015). Characterisation of nanoparticle emissions and exposure at traffic intersections through fast–response mobile and sequential measurements. *Atmospheric Environment, 107*, 374–390.

Gong, X., Zhang, C., Chen, H., Nizkorodov, S. A., Chen, J., & Yang, X. (2016). Size distribution and mixing state of black carbon particles during a heavy air pollution episode in Shanghai. *Atmospheric Chemistry and Physics, 16*, 5399–5411.

Hansen, A. D. A., Rosen, H., & Novakov, T. (1984). The aethalometer—an instrument for the real-time measurement of optical absorption by aerosol particles. *The Science of the Total Environment, 36*, 191–196.

Jing, H., Li, Y. F., Zhao, J., Li, B., Sun, J., Chen, R., & Chen, C. (2014). Wide-range particle characterization and elemental concentration in Beijing aerosol during the 2013 Spring Festival. *Environmental Pollution, 192*, 204–211.

Joshi, M., Khan, A., Anand, S., & Sapra, B. K. (2016). Size evolution of ultrafine particles: Differential signatures of normal and episodic events. *Environmental Pollution, 208*, 354–360.

Kumar, M., Singh, R. S., and Banerjee, T. (2015). Associating airborne particulates and human health: exploring possibilities: comment on: Kim, Ki-Hyun, Kabir, E. and Kabir, S. 2015. A review on the human health impact of airborne particulate matter. Environment International 74 (2015) 136-143. *Environment international, 84*, 201.

Kumar, M., Singh, R. K., Murari, V., Singh, A. K., Singh, R. S., & Banerjee, T. (2016). Fireworks induced particle pollution: a spatio-temporal analysis. *Atmospheric Research, 180*, 78–91.

Kumar, M., Raju, M. P., Singh, R. K., Singh, A. K., Singh, R. S., & Banerjee, T. (2017a). Wintertime characteristics of aerosols over middle Indo-Gangetic Plain: vertical profile, transport and radiative forcing. *Atmospheric Research, 183*, 268–282.

Kumar, M., Raju, M. P., Singh, R. S., & Banerjee, T. (2017b). Impact of drought and normal monsoon scenarios on aerosol induced radiative forcing and atmospheric heating in Varanasi over middle Indo-Gangetic Plain. *Journal of Aerosol Science, 113*, 95–107.

Lelieveld, J., Evans, J. S., Fnais, M., Giannadaki, D., & Pozzer, A. (2015). The contribution of outdoor air pollution sources to premature mortality on a global scale. *Nature, 525*, 367–371.

Lin, C. C., Huang, K. L., Chen, H. L., Tsai, J. H., Chiu, Y. P., Lee, J. T., & Chen, S. J. (2014). Influences of beehive firework displays on ambient fine particles during the Lantern Festival

in the YanShuei area of southern Taiwan. *Aerosol and Air Quality Research, 14*(7), 1998–2009.

Liu, D. Y., Rutherford, D., Kinsey, M., & Prather, K. A. (1997). Real-time monitoring of pyrotechnically derived aerosol particles in the troposphere. *Analytical Chemistry, 69*, 1808–1814.

Mhawish, A., Banerjee, T., Broday, D. M., Misra, A., & Tripathi, S. N. (2017). Evaluation of MODIS Collection 6 aerosol retrieval algorithms over Indo-Gangetic Plain: implications of aerosols types and mass loading. *Remote Sensing of Environment, 201*, 297–313.

Mhawish, A., Kumar, M., Mishra, A.K., Srivastava, P.K., Banerjee, T. (2018). Remote sensing of aerosols from space: retrieval of properties and applications. In. Remote Sensing of Aerosols, Clouds, and Precipitation. Elsevier Inc, 1-38. https://doi.org/10.1016/B978-0-12-810437-8.00003-7.

Moreno, T., Querol, X., Alastuey, A., Minguillón, M. C., Pey, J., Rodriguez, S., & Gibbons, W. (2007). Recreational atmospheric pollution episodes: inhalable metalliferous particles from firework displays. *Atmospheric Environment, 41*, 913–922.

Murari, V., Kumar, M., Barman, S. C., & Banerjee, T. (2015). Temporal variability of MODIS aerosol optical depth and chemical characterization of airborne particulates in Varanasi, India. *Environmental Science and Pollution Research, 22*, 1329–1343.

Murari, V., Kumar, M., Singh, N., Singh, R. S., & Banerjee, T. (2016). Particulate morphology and elemental characteristics: variability at middle Indo-Gangetic Plain. *Journal of Atmospheric Chemistry, 73*, 165–179.

Murari, V., Kumar, M., Mhawish, A., Barman, S. C., & Banerjee, T. (2017). Airborne particulate in Varanasi over middle Indo-Gangetic Plain: variation in particulate types and meteorological influences. *Environmental Monitoring and Assessment, 189*, 157–171.

Perrino, C., Tiwari, S., Catrambone, M., Dalla Torre, S., Rantica, E., & Canepari, S. (2011). Chemical characterization of atmospheric PM in Delhi, India, during different periods of the year including Diwali festival. *Atmospheric Pollution Research, 2*, 418–427.

Ramanathan, V. C. P. J., Crutzen, P. J., Kiehl, J. T., & Rosenfeld, D. (2001). Aerosols, climate, and the hydrological cycle. *Science, 294*, 2119–2124.

Retama, A., Neria-Hernández, A., Jaimes-Palomera, M., Rivera-Hernández, O., Sánchez-Rodríguez, M., López-Medina, A., & Velasco, E. (2019). Fireworks: a major source of inorganic and organic aerosols during Christmas and New Year in Mexico city. *Atmospheric Environment: X, 2*, 100013.

Sarkar, S., Khillare, P. S., Jyethi, D. S., Hasan, A., & Parween, M. (2010). Chemical speciation of respirable suspended particulate matter during a major firework festival in India. *Journal of Hazardous Materials, 184*, 321–330.

Seidel, D. J., & Birnbaum, A. N. (2015). Effects of Independence Day fireworks on atmospheric concentrations of fine particulate matter in the United States. *Atmospheric Environment, 115*, 192–198.

Sen, A., Abdelmaksoud, A. S., Ahammed, Y. N., Banerjee, T., Bhat, M. A., Chatterjee, A., & Gadi, R. (2017). Variations in particulate matter over Indo-Gangetic Plains and Indo-Himalayan Range during four field campaigns in winter monsoon and summer monsoon: role of pollution pathways. *Atmospheric Environment, 154*, 200–224.

Sharma, S. K., Kumar, M., Rohtash, Gupta, N. C., Saraswati, Saxena, M., & Mandal, T. K. (2014). Characteristics of ambient ammonia over Delhi, India. *Meteorology and Atmospheric Physics, 124*, 67–82.

Singh, R. P., Dey, S., & Holben, B. (2003). Aerosol behaviour in Kanpur during Diwali festival. *Current Science, 84*, 1302–1304.

Singh, N., Mhawish, A., Deboudt, K., Singh, R. S., & Banerjee, T. (2017). Organic aerosols over Indo-Gangetic Plain: Sources, distributions and climatic implications. *Atmospheric Environment, 157*, 59–74.

Thakur, B., Chakraborty, S., Debsarkar, A., Chakrabarty, S., & Srivastava, R. C. (2010). Air pollution from fireworks during festival of lights (Deepawali) in Howrah, India-a case study. *Atmosfera, 23*, 347–365.

Tritscher, T., Koched, A., Han, H. S., Filimundi, E., Johnson, T., Elzey, S., & Bischof, O. F. (2015). Multi-instrument manager tool for data acquisition and merging of optical and electrical mobility size distributions. In Journal of Physics: Conference Series (Vol. 617, No. 1, p. 012013). IOP Publishing.

Vecchi, R., Bernardoni, V., Cricchio, D., D'Alessandro, A., Fermo, P., Lucarelli, F., & Valli, G. (2008). The impact of fireworks on airborne particles. *Atmospheric Environment, 42*, 1121–1132.

Virkkula, A., Mäkelä, T., Hillamo, R., Yli-Tuomi, T., Hirsikko, A., Hämeri, K., & Koponen, I. K. (2007). A simple procedure for correcting loading effects of aethalometer data. *Journal of the Air & Waste Management Association, 57*, 1214–1222.

Wang, Y., Zhuang, G., Xu, C., & An, Z. (2007). The air pollution caused by the burning of fireworks during the lantern festival in Beijing. *Atmospheric Environment, 41*, 417–431.

Wen, L., & Chen, J. (2013). Severe aerosol pollution derived from fireworks: a case in Jinan, China. *JSM Environmental Science & Ecology, 1*, 1004.

Yamada, M., Takaya, M., & Ogura, I. (2015). Performance evaluation of newly developed portable aerosol sizers used for nanomaterial aerosol measurements. *Industrial Health*, 2014–0243.

Zhang, M., Wang, X., Chen, J., Cheng, T., Wang, T., Yang, X., & Chen, C. (2010). Physical characterization of aerosol particles during the Chinese New Year's firework events. *Atmospheric Environment, 44*, 5191–5198.

Zhao, S., Yu, Y., Yin, D., & He, J. (2017). Effective density of submicron aerosol particles in a typical valley city, western China. *Atmospheric Pollution Research, 17*, 1–13.